Patria and Putra *Geosci. Lett. (2020) 7:1*
https://doi.org/10.1186/s40562-020-0150-2

Geoscience Letters

RESEARCH LETTER

Open Access

Development of the Palu–Koro Fault in NW Palu Valley, Indonesia

Adi Patria* and Purna Sulastya Putra

Abstract

The 220-km-long Palu–Koro Fault, Central Sulawesi, is a major fault with prominent expression in Eastern Indonesia. Many studies about the Palu–Koro Fault have shown its capability of generating large earthquakes, but how the Palu–Koro Fault has evolved remains enigmatic. This study is to investigate the geomorphology of NW Palu Valley based on DEMNAS (Digital Elevation Model of Indonesia) and field observations to understand the development of the Palu–Koro Fault. The study area comprises a high mountain in the west and a valley in the east. There are two major normal faults and a strike–slip fault observed in NW Palu Valley. The western normal fault is a basin-bounding fault, which marks the topographic break between mountain and valley. To the east, another normal fault is observed cutting the old alluvial fans and expressed by planar fault scarps. The strike–slip fault is observed within the basin and crosses the distal part alluvial fans. It is expressed by intra-basin ridges in places which are slightly uplifted from the adjacent surface. The surface rupture of the 2018 Mw 7.5 Palu earthquake in NW Palu Valley also shows left-lateral movement up to 4 m. We consider that the development of the Palu–Koro Fault in NW Palu Valley is characterized by toward-central-basin migration of faulting activity from basin-bounding fault to intra-basin fault.

Keywords: Palu–Koro Fault, Active tectonics, Tectonic geomorphology

Introduction

Sulawesi is located at the triple junction where the Pacific, Australian, and Eurasian plates converge, and it also records a complex geological history of subduction, extension, obduction, and collision (e.g., Hamilton 1979; Silver et al. 1983; Hall and Wilson 2000; Hinschberger et al. 2005; Hall 2002, 2012, 2018; Nugraha and Hall 2018). Sulawesi is a seismically active region where earthquakes with a magnitude greater than 4.5 and a depth less than 30 km are dominantly observed in Central Sulawesi and offshore North Sulawesi (Fig. 1a).

The Palu–Koro Fault is the major active fault in Central Sulawesi with left-lateral movement and a NNW–SSE trend (Katili 1970; Tjia 1978; Hamilton 1979; Bellier et al. 2001; Daryono 2016; Watkinson and Hall 2017). It can be recognized based on its prominent expression spanning from Palu to North Luwu Regency along 220 km. The fault is a major boundary and accommodates the 42 mm year^{-1} relative motion between the Makassar Block and the North Sula Block (Socquet et al. 2006). It was also interpreted to be connected to the Matano Fault at its southern end (Hamilton 1979; Bellier et al. 2001; Socquet et al. 2006; Daryono 2016; Fig. 1a). The Palu–Koro and Matano faults have been reactivated due to the Mid-Pliocene collision in an E–W direction between the East Sulawesi and the Banggai Sula Blocks in the eastern arm of Sulawesi (Villeneuve et al. 2002; Bellier et al. 2006). Both faults accommodate left-lateral slip transferred from the E–W convergence (Bock et al. 2003; Socquet et al. 2006). To the north, the Palu–Koro Fault continues along offshore and terminates at the west end of the North Sulawesi Subduction (Hamilton 1979; Rangin et al. 1999; Hall and Wilson 2000; Fig. 1a). The convergence rate of the subduction increases toward west from 20 to 54 mm year^{-1}, resulting from a clockwise rotation of North Sulawesi about a pole located at the NE Sulawesi (Silver et al. 1983; Walpersdorf et al. 1998; Stevens et al. 1999; Rangin et al. 1999; Bock et al. 2003).

*Correspondence: adi.patria@lipi.go.id
RC for Geotechnology, Indonesian Institute of Sciences (LIPI), Bandung, Indonesia

Seismicity analysis indicates that the Palu–Koro Fault remains active with clustered source locations, and the faulting activity is dominated by strike–slip, normal, and thrust faults earthquakes (Pakpahan et al. 2015). The fault is also known as it has the greatest seismic risk in Eastern Indonesia and is capable of generating large earthquake (Bellier et al. 1998; Walpersdorf et al. 1998; Stevens et al. 1999; Daryono 2016; Watkinson and Hall 2017; Cipta et al. 2017). Indeed, on 28th of September 2018, an Mw 7.5 earthquake occurred and ruptured the fault with up to 7 m left-lateral offset, extending 180 km and traversing Palu City (Bao et al. 2019; Socquet et al. 2019). It was shortly followed by a 4- to 7-m-high tsunami, possibly associated with submarine landslides (Putra et al. 2019; Sassa and Takagawa 2019; Takagi et al. 2019). According to many earthquake catalogs (e.g., United States Geological Survey (USGS); Indonesian Meteorological, Climatological, and Geophysical Agency (BMKG); German Research Centre for Geosciences (GFZ); Global Centroid-Moment-Tensor (GCMT)), the hypocenter was located in Donggala Regency, about 80 km to the north from Palu City and at a depth of 10–15 km.

Although many studies have been undertaken concerning the Palu–Koro Fault, its development remains enigmatic. This study aims to interpret the tectonic geomorphology based on field investigation, including some recent surface rupture and digital elevation data of Indonesia (DEMNAS) along the NW Palu Valley that shows geomorphic evidence of faulting and its relative timing, then we also propose the evolutionary model of Palu–Koro Fault in NW Palu Valley.

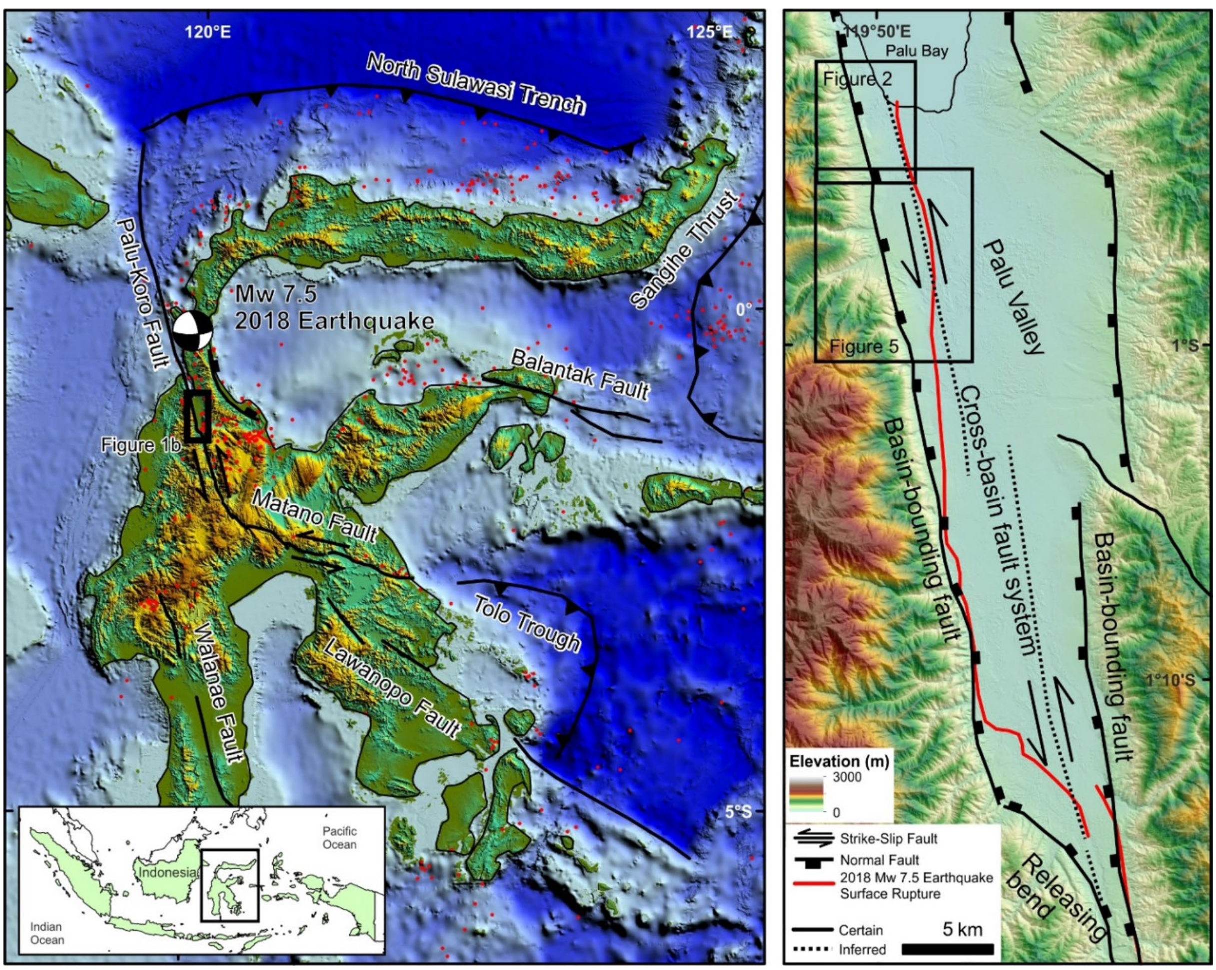

Fig. 1 **a** Tectonic map of Sulawesi showing major structures in the region (compiled from Hamilton 1979; Hall and Wilson 2000; Hinschberger et al. 2005; Hall 2012). Red dots indicate earthquake hypocenters with a magnitude greater than 4.5 and a depth less than 30 km between 1980 and 2016. Moment tensor of the Mw 7.5 2018 earthquake and earthquake hypocenters are from the USGS Earthquake Catalog. **b** DEM map showing morpho-structural elements of Palu Basin. Palu Valley is bounded by two mountains in the East and West. Structural elements in Palu Valley are compiled from previous authors (e.g., Bellier et al. 2001; Watkinson and Hall 2017; Socquet et al. 2019)

Tectonic setting

Palu Valley was formed due to transtensional tectonic associated with the Palu–Koro Fault (Bellier et al. 2001, 2006). The valley is bounded by high mountains trending N–S in the east and the west, reaching an elevation of 2.3 km (Fig. 1b). The high mountains dominantly consist of metamorphic complexes and granitic rocks (Sukamto et al. 1973). Bellier et al. (1999) noted two distinct alluvial fan units within the western part of Palu Valley with abandonment ages of ~11 kya and ~120 kya, respectively, for young and old alluvial fan units, or during the last two humid periods after termination of global glacial stages. The western mountain is characterized by a highly linear scarp with geomorphic features in its central part, majorly showing normal faulting evidence, while the eastern mountain is relatively more eroded and segmented (Watkinson and Hall 2017; Fig. 1b). To the south, the Palu–Koro Fault traverses to a narrow valley, and the fault segments are linked by a NW–SE trending releasing bend (Bellier et al. 2001; Watkinson and Hall 2017). The movement of the fault is mostly indicated by left-lateral stream offsets, observed in the northern and southern part of the fault (Bellier et al. 1998, 2001; Watkinson and Hall 2017).

Bellier et al. (2001) estimated that the Holocene slip rate of the Palu–Koro Fault is 35 ± 8 mm $year^{-1}$ based on cumulative stream offset and age of young alluvial fan from ^{10}Be cosmogenic dating. GPS measurement from Walpersdorf et al. (1998) suggests a left-lateral slip rate of 34 mm $year^{-1}$ with 4 mm $year^{-1}$ in normal component, and Stevens et al. (1999) estimated a slip rate of 38 ± 8 mm $year^{-1}$ with a locking depth of 2–8 km. Socquet et al. (2006) also calculated the total motion of 40 mm $year^{-1}$ with four parallel strands, which are locked at a depth of 0–5 km. These geodetic measurements from many studies have confirmed the fast slip rate of the Palu–Koro Fault.

Paleoseismology work from Bellier et al. (1998) revealed that there were three Mw 6.8–8 earthquakes during the last 2000 years with a recurrence interval of about 700 years. If each earthquake had 10 m lateral displacement, the total slip should total 30 m for 2000 years. This total displacement is less than the predicted cumulative slip of 54–86 m for 2000 years if the slip rate is 35 ± 8 mm $year^{-1}$. Thus Bellier et al. (2001) argued a creeping mechanism for the Palu–Koro Fault. Alternatively, Watkinson and Hall (2017) proposed that a cross-basin strike–slip fault system, which is possibly covered by

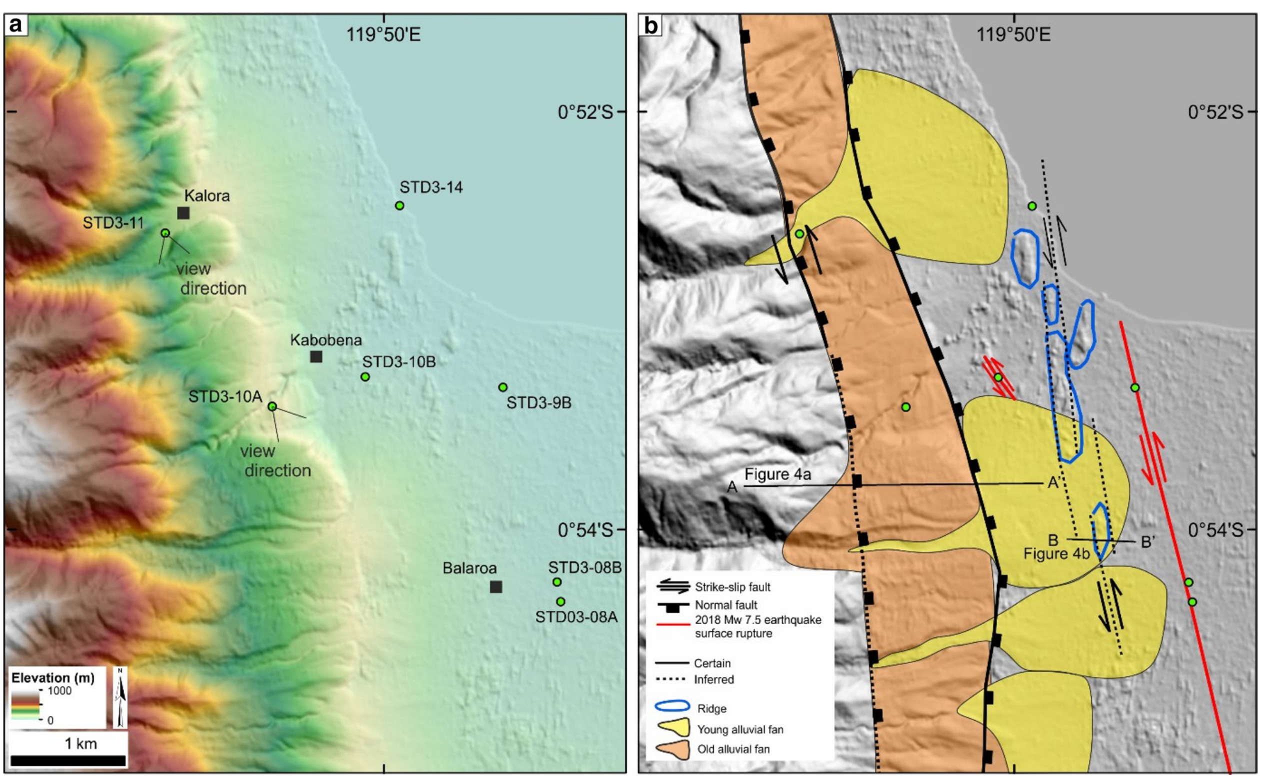

Fig. 2 **a** DEM map showing the geomorphology of the North Area and observation sites. **b** Interpretation of DEMNAS combined with field observation on a hillshade image showing geomorphic features of the area

fluvial deposits and lacks clear geomorphic expression, accommodates the lateral slip deficit. Daryono (2016) also observed that the recent activity of the fault in the northern Palu Valley is expressed by fresh morphology in the middle of the valley, and the western sidewall fault in the northern part of the fault is inactive.

Prior to 2018, the Palu–Koro Fault was characterized by low-level seismicity (McCaffrey and Sutardjo 1982; Bellier et al. 2001). Pakpahan et al. (2015) proposed that seismicity in the Palu Valley is clustered because of the segmentation of the fault and some minor faults. Katili (1970) mentioned that three destructive earthquakes in 1905, 1907, and 1934 were related to the Palu–Koro Fault activity. Based on USGS Catalog, significant earthquakes occurred close to the Palu–Koro Fault in 1968 (Mw 6.7), 1998 (Mw 6.7 and 6), 2005 (Mw 6.3), 2012 (Mw 6.3), and 2018 (Mw 7.5 and 6.1). The 2018 Mw 7.5 Palu earthquake had a strike–slip solution and caused damage to Palu City, Donggala Regency, and Sigi Regency. An Mw 6.1 foreshock occurred before the Mw 7.5 earthquake,

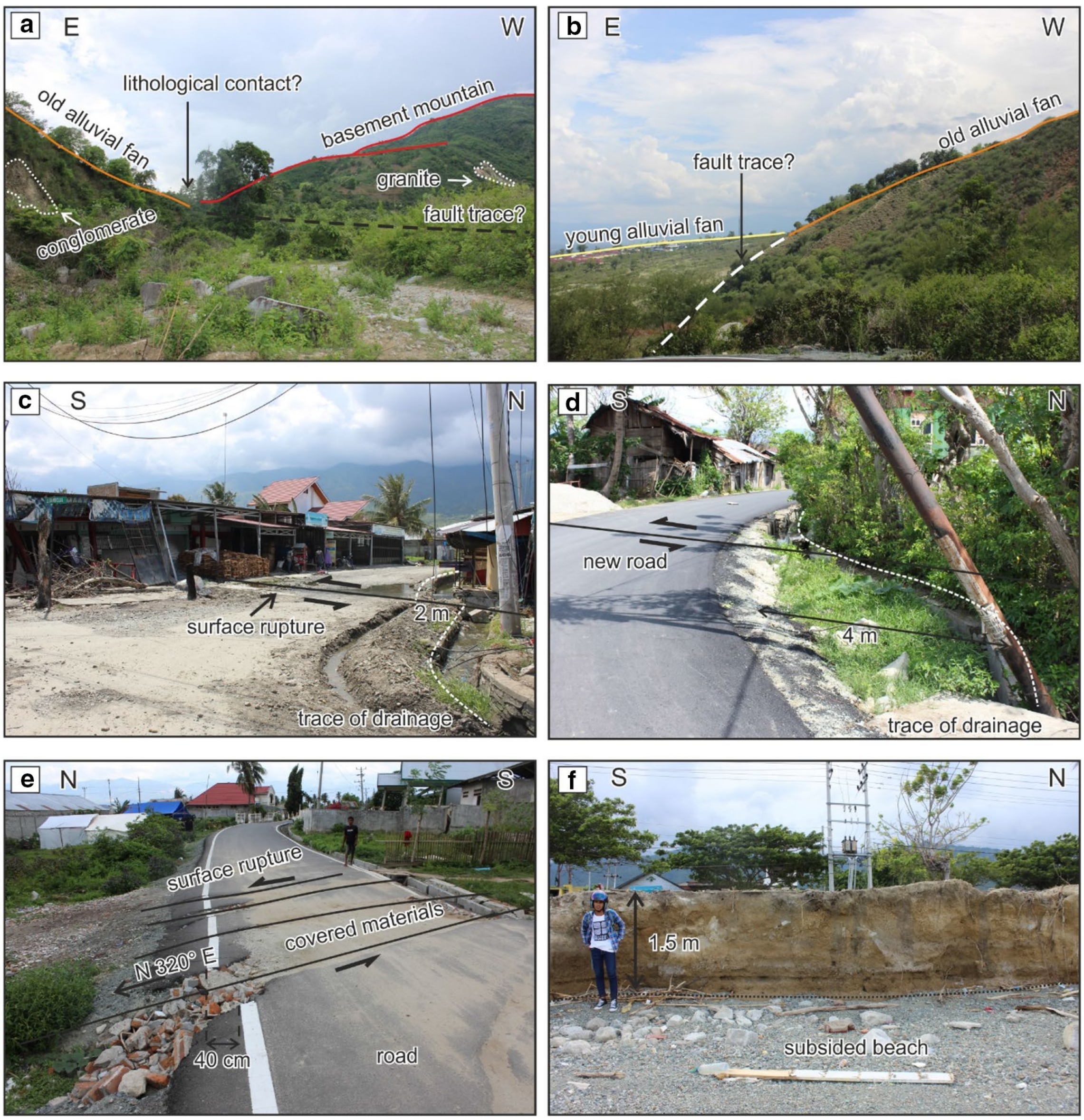

Fig. 3 **a** A view from STD3-11 showing contact between granite in mountain and conglomerate further east. A depression in between is interpreted as a basin-bounding fault. **b** A view from STD3-10A showing the relationship between old and young alluvial fan units. A topographic break may indicate a normal fault. **c**, **d** Major surface rupture with left-lateral displacement close to Balaroa at STD3-08B and STD3-9B, respectively. **e** Minor surface rupture at STD3-10B showing left-lateral displacement. **f** Subsided surface on the beach at STD3-14

followed by several aftershock earthquakes. The surface rupture was sharp and straight along Palu Valley with the rupture velocity of 4.3–5.2 km/s, thus the event has been classified as a supershear earthquake (Bao et al. 2019; Socquet et al. 2019).

Methodology

Publicly available digital elevation data of Indonesia (DEMNAS) from Geospatial Information Agency of Indonesia (BIG) are used in this study. DEMNAS is available for the whole Indonesian region with 0.27 arcsecond or about 8.3 m spatial resolution. Interpretation of DEMNAS is made to investigate the geomorphology of the western mountain and alluvial fans. This study is also based on field investigation to examine the relationship of geomorphic features, including the surface ruptures associated with the 2018 Palu earthquake. The results from DEMNAS and field observations are combined to produce an evolutionary model of the Palu–Koro Fault.

Results

North area

Topographically, the northern part of the study area is characterized by a mountain in the west and low-lying plains in the east (Fig. 2a). There are two distinct alluvial fan units observed in this area (Fig. 2b). The old alluvial fan unit is bounded by a mountain in the west and elongates in a NNW–SSE direction. It was overlapped by feeder channels of the young alluvial fan unit, which is located east of the old alluvial fan unit. A young alluvial fan is observed in the east of Kalora Village with the axis of the fan, which is slightly deflected to the north from its feeder channel (Fig. 2b). In the field, at the bend of the feeder channel (STD3-11), a lithological change from granite in the mountain to conglomerate in the hill may indicate a basin-bounding fault contact in between (Fig. 3a). The relationship of both alluvial fan units is also clearly shown in the south of Kabobena where the young alluvial fan truncates the old alluvial fan (Fig. 3b). Both alluvial fans are separated

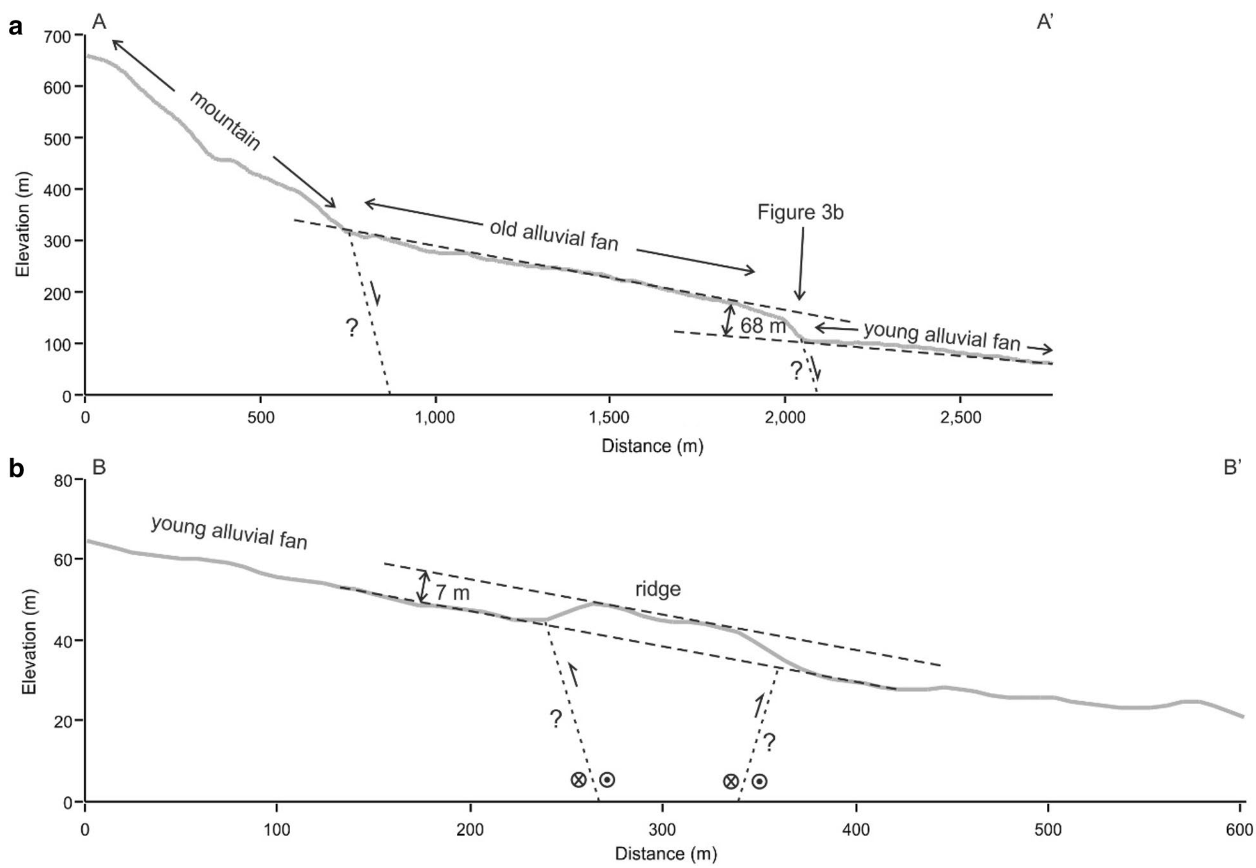

Fig. 4 **a** Profile A–A′ showing the topography from the mountain to the young alluvial fan. A topographic break between mountain and an old alluvial fan may mark the basin-bounding fault. A scarp separating old and young alluvial fans is interpreted as a normal fault. **b** Profile B–B′ of an intra-basin ridge, which emerges from adjacent topography on a young alluvial fan. See Fig. 2 for the location of profiles

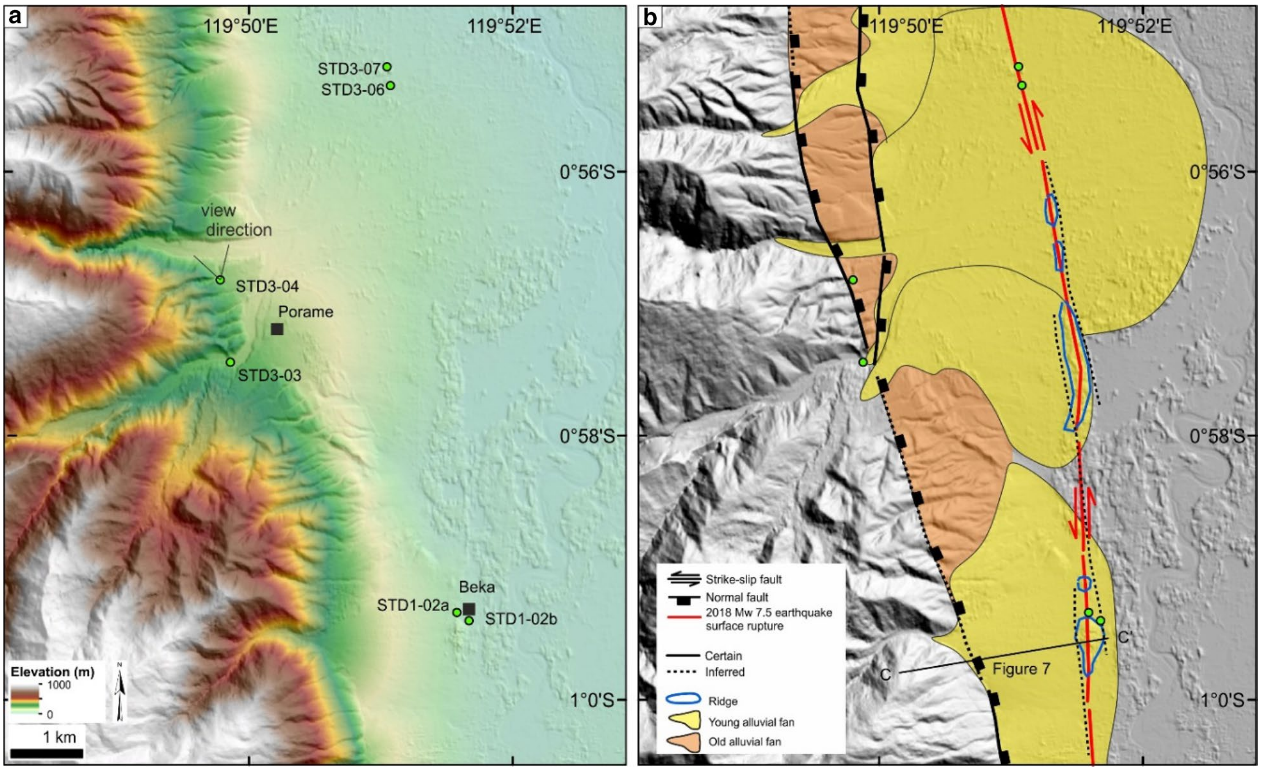

Fig. 5 **a** DEM map showing the geomorphology of the South Area and observation sites. **b** Interpretation of DEMNAS combined with field observation on a hillshade image showing geomorphic features of the area

by a 68-m linear topographic break, which may represent a normal fault scarp (Figs. 3b and 4a).

North of Balaroa, a ridge on the young alluvial fan with a NNW–SSE orientation is elevated about 7 m above adjacent ground (Figs. 2b and 4b). A series of ridges with a similar trend can also be observed further north till reaching the coastline. Transpressional deformation related to the Palu–Koro Fault may be responsible for the formation of the ridges.

We also observed surface deformation associated with the 2018 Palu earthquake. Evidence of the major surface rupture is shown in several locations in the western part of Palu City (STD3-8A, STD3-8B, and STD3-9B), showing a left-lateral displacement up to 4 m along a N 350°E direction (Fig. 3c, d). Further west from the major surface rupture, on STD3-10B, a road was offset 60 cm with several minor strike–slip displacements trending N320°E, which are considered as a minor surface rupture (Fig. 3e). We also observed a subsided beach with a vertical displacement of 1.5 m on STD3-14 (Fig. 3f).

South area

To the west of the mountain, we observed old and young alluvial fan units, but the old alluvial fan unit disappears further toward the south (Fig. 5a, b). East of Porame Village, there are two young alluvial fans. The younger alluvial fan deposition seems to be deflected to the north and partly overlies the other alluvial fan (Fig. 5b). At STD3-03, the lithological change from the phyllite and alluvial fan deposit was observed on the river (Fig. 6a). To the south of the river, the alluvial fan deposit shows a horizontal stratification (Fig. 6b). The basement rock of phyllite is observed in contact with the alluvial fan deposit, and it is intensively sheared (Fig. 6c). The sheared phyllite appears as a damage zone of the fault, thus we interpret the contact as a basin-bounding fault. Further north, at STD3-04, the evidence of normal faulting can also be reflected by the geometry of the old alluvial fan deposit, which shows thickening-toward-fault geometry (Fig. 6d). The basin-bounding fault is also marked by the topographic break between the mountain and the old alluvial fan unit. Topographic highs that emerge above the adjacent surface with a N–S direction are observed at the distal part of the young alluvial fan unit in the west of Porame, suggesting pop-up deformation after deposition of alluvial fans. This series of ridges was also cut by the 2018 surface rupture (Fig. 5b).

Beka Village is located on the distal part of a young alluvial fan. The alluvial fan is sized about 2.5 km N–S

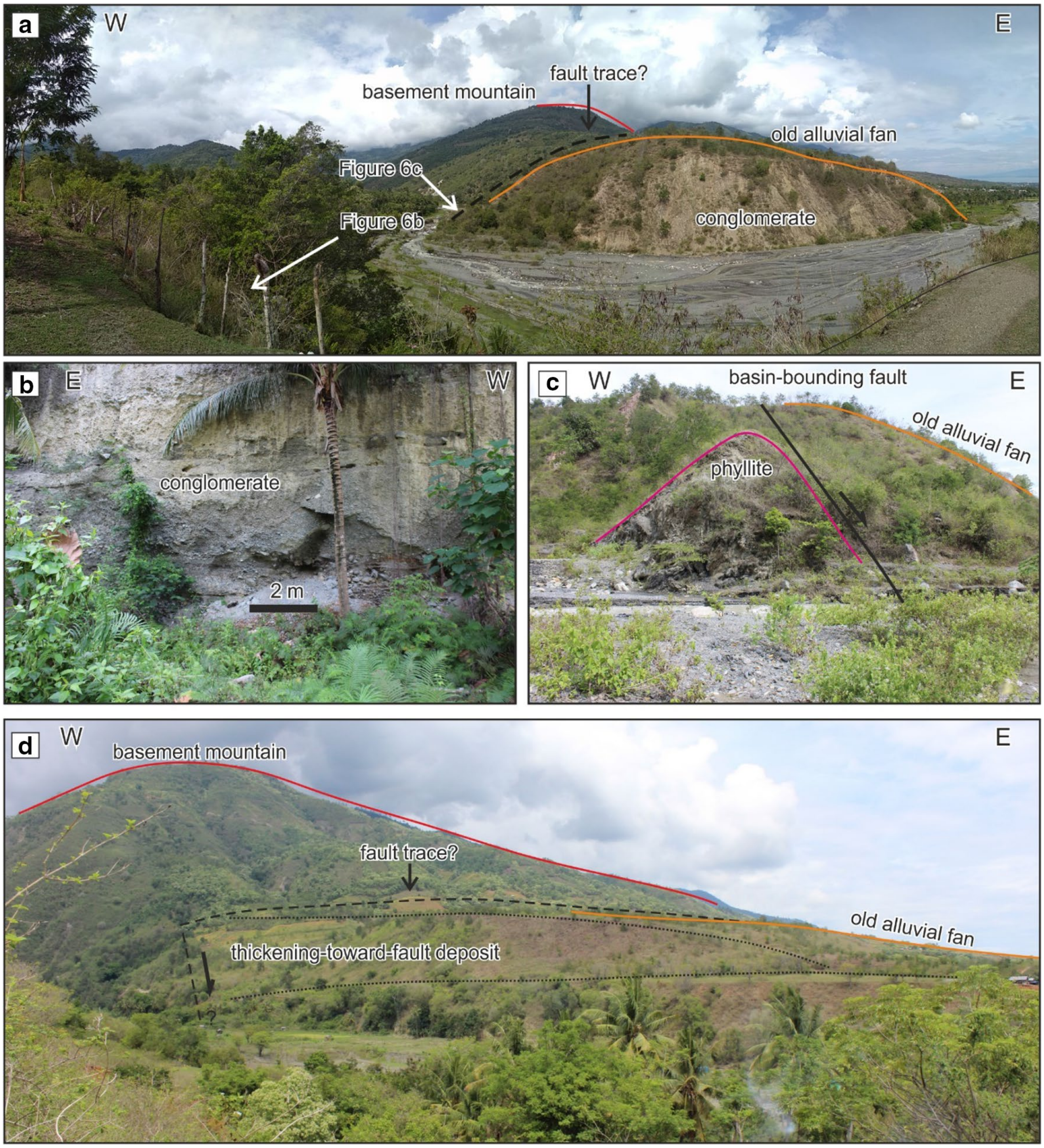

Fig. 6 **a** Geomorphology of the western mountain, which consists of phyllite and the old alluvial fan in the west of Porame, STD3-03. **b** Horizontal strata of the old alluvial fan deposit. **c** Exposure of contact between phyllite and old alluvial fan deposit. Phyllite is situated at the footwall and highly sheared. **d** A view from STD3-04 showing morphology of mountain and old alluvial fan. The appearance of an old alluvial fan indicates a thickening-toward-fault deposit

and 2.2 km E–W. It gives a clear topographic break between the mountain and the alluvial fan. Thus, we interpreted that a normal fault may control the deposition of the alluvial fan (Figs. 5b and 7). At the distal part of the alluvial fan, the topography is slightly uplifted, forming a ridge with a N–S trend, and the 22 m rise of the ground is possibly due to transpressional deformation (Fig. 7). Coincidentally, the surface rupture of the 2018 Palu earthquake was observed crossing this ridge in a parallel direction to the ridge orientation.

Two distinct surface ruptures of the 2018 Palu earthquake can be observed in Beka Village, shown in Fig. 8. The first is a major surface rupture, which is located in the west of Beka Village. Evidence of left-lateral

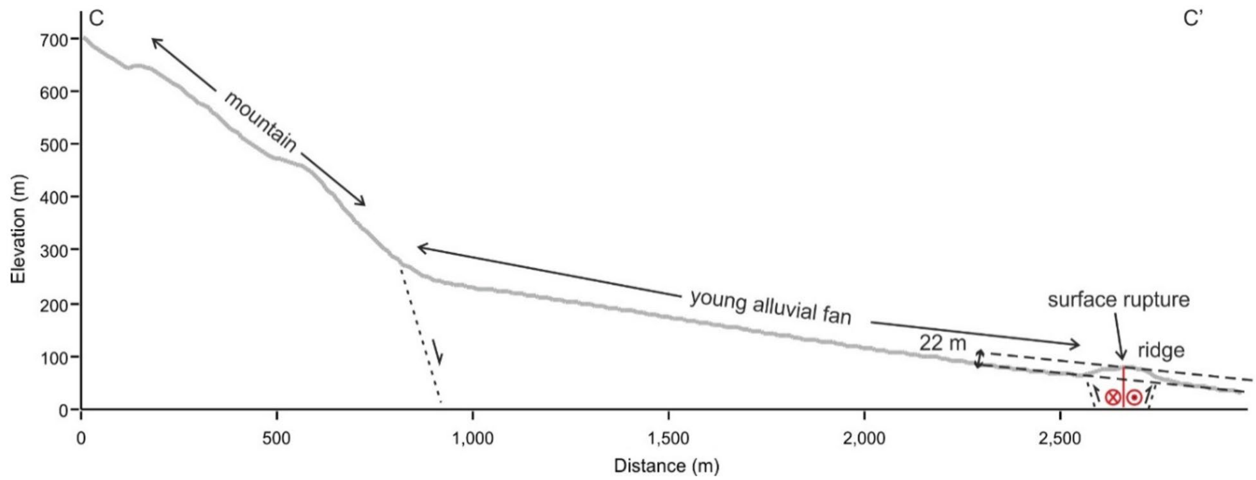

Fig. 7 Profile C–C′ showing the topography from the mountain to the young alluvial fan. Topographic break marks the basin-bounding fault, and a ridge is elevated 22 m from the adjacent surface. The ridge coincides with the major surface rupture of the 2018 Palu earthquake. See Fig. 5 for the location of the profile

strike–slip faulting is clearly seen by 2 m offset of the road (Fig. 8b). The surface rupture is oriented along a N–S direction. Just north of the road offset, the ground is uplifted 50–70 cm (Fig. 8c), and in contrast, to the south of road offset, subsided ground indicates 70–100 cm vertical displacement (Fig. 8d). Although Beka Village is situated 150 m east of the major surface rupture, the village also experienced minor surface deformation. The surface deformation indicates normal faulting with 1 m separation and a horizontal slip component of 20 cm (Fig. 8e, f). The normal faults, which connected with a relay ramp have a relatively parallel trend with the major rupture. The normal faults elongate about 200 m and cannot be traced further north and south.

Discussion

The dynamics of the Palu–Koro Fault are well recorded in the field and expressed by geomorphic features. There are at least three major faults in the NW Palu Valley. A basin-bounding fault is marked by a clear topographic break acting as the mountain front. The topographic break also marks the truncation of the old alluvial fan unit. The deposition of old alluvial fans was controlled by the basin-bounding fault, indicated by a thickening-toward-fault deposit. The basin-bounding faulting activity seems to have ended at 120 kya (Fig. 9a), suggested by the age of abandonment of the old alluvial fan unit (Bellier et al. 1999). Then the faulting activity migrated to the east along the distal part of the old alluvial fan unit. The migration has initiated the deposition of young alluvial fans further to the east, which onlaps to the old alluvial fans (Fig. 9b). Bellier et al. (1999) measured that the young alluvial fans were abandoned at 11 kya.

Younger faulting activity is mainly expressed by deformation at the distal parts of young alluvial fans in which has formed N–S oriented ridges (Fig. 9c). A series of ridges are uplifted from adjacent topography, indicating young localized uplift, which is plausible as a result of strike–slip faulting. This deformation gives clear evidence that the recent activity of the Palu–Koro Fault is accommodated by intra-basin faulting. This observation agrees with interpretations from Daryono (2016), which suggests that faulting activity is expressed by fresh morphology within the basin in the north Palu Valley.

Our field survey along NW Palu Valley has identified a major surface rupture with up to 4 m left-lateral offset, associated with the 2018 Palu earthquake. This observation is in agreement with the result from satellite imagery processing that shows 4–7 m displacement (Socquet et al. 2019). The major surface rupture is evidence of the recent activity of intra-basin strike–slip faulting. Additionally, there are also minor surface ruptures associated with the 2018 Palu earthquake. A minor strike–slip surface rupture, close to Kabobena Village, could be an upward splay of the major rupture, or alternatively, there may be a buried synthetic fault that was also ruptured during the 2018 earthquake. Another minor surface rupture with a major normal slip component in Beka Village is interpreted as a result of gravitational collapse since it is parallel to the major surface rupture and has a limited extent.

The migration of faulting activity has been previously proposed by Watkinson and Hall (2017), and they inferred that the cross-basin fault diagonally elongates from the narrow valley, close to the releasing bend, till Palu Bay. However, we consider that the progressive migration of faulting activity from the basin-bounding

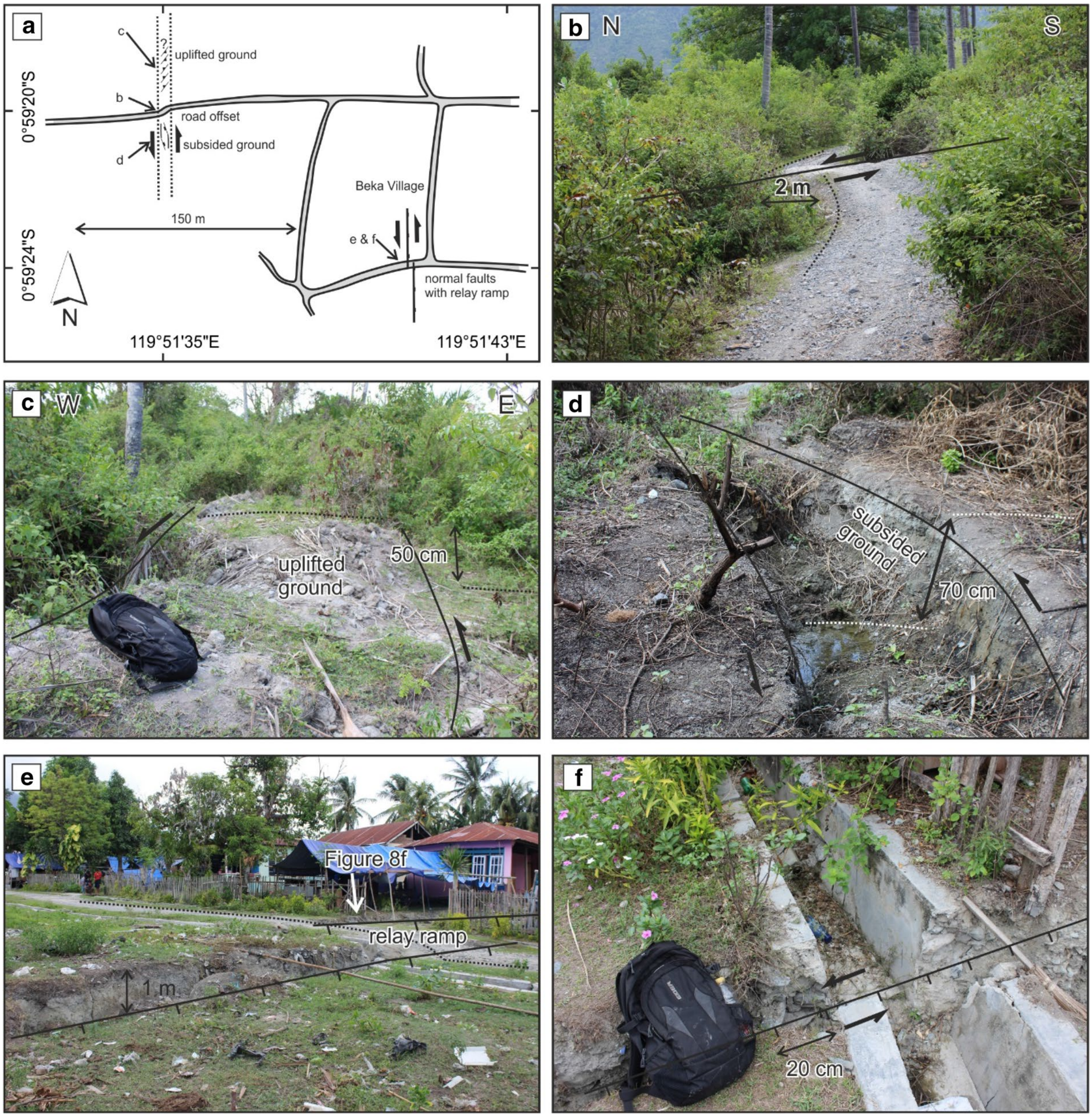

Fig. 8 **a** Surface rupture of the 2018 Palu earthquake in Beka Village. **b** A 2-m left-lateral offset village road. **c** The ground was uplifted 50 cm above the adjacent surface. **d** Subsided ground with rhombic shape. **e** Normal faults with a maximum throw of 1 m, connected with relay ramp. **f** Close view of a normal fault, the fault has a minor strike–slip component of 20 cm

fault toward the cross-basin fault has also occurred in the NW Palu Valley. The migration of faulting activity toward basin center was also observed in other strike–slip fault systems in the world, such as Haiyuan Fault Zone (Zhang et al. 1989), Enriquillo-Plantain Garden–Walton Fault (Mann et al. 1995), and Kyaukkyan Fault (Crosetto et al. 2018). The migration might be caused by the tendency of strike–slip faults to straighten (Zhang et al. 1989; Wu et al. 2009).

Conclusions

The dynamics of the Palu–Koro Fault are recorded in the geomorphology of NW Palu Valley. The topographic break between the western mountain and Palu Valley indicates a major basin-bounding fault that controlled the deposition of old alluvial fans. Fault scarps along the eastern part of old alluvial fans represent normal faulting activity, which initiated the deposition of young alluvial fans. Intra-basin strike–slip faulting, which deforms

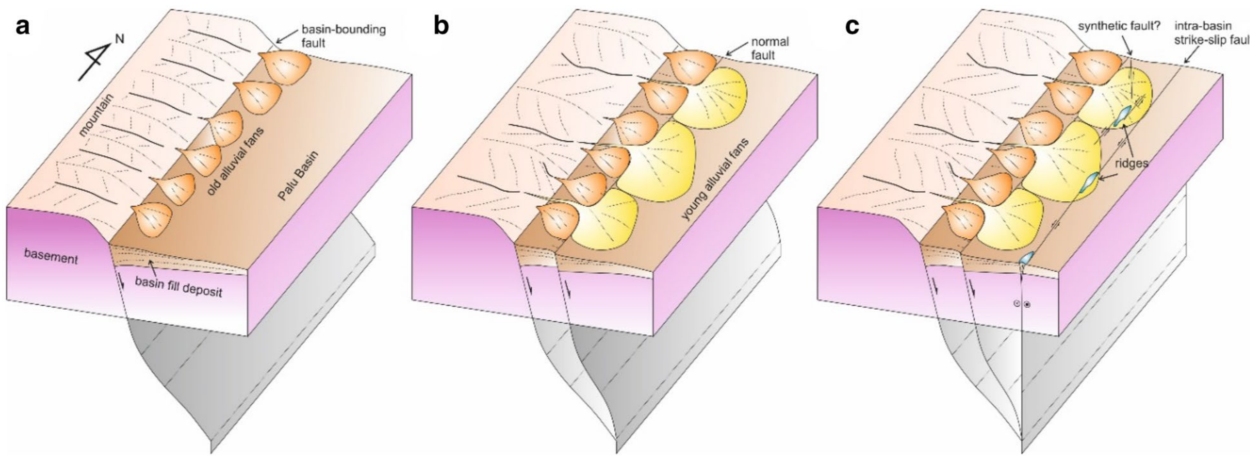

Fig. 9 A schematic evolutionary model of the Palu–Koro Fault in NW Palu Valley with age of abandonments for two alluvial fan units from Bellier et al. (1999). **a** Deposition of old alluvial fans, controlled by a basin-bounding fault, which has a major normal slip component. This phase may end at 120 kya. **b** The episode of later normal faulting in the east, triggered the deposition of young alluvial fans, which truncated against the old alluvial fans. These alluvial fans were displaced at 11 kya. **c** Later deformation is dominated by strike–slip faulting. A series of N–S ridges uplifted distal parts of some young alluvial fans and may be associated with transpression deformation. This strike–slip fault was ruptured during the 2018 Palu earthquake

distal portions of the young alluvial fans, is expressed by a series of N–S trending ridges. The 2018 earthquake also indicates the intra-basin strike–slip faulting activity in NW Palu Valley. The development of the Palu–Koro Fault in NW Palu Valley is characterized by the eastward progressive migration of faulting activity from the basin-bounding fault to a more easterly normal fault and, most recently, to the intra-basin strike–slip fault.

Acknowledgements
We thank RC for Geotechnology LIPI and its staff for the support. We thank Eko Yulianto for the supervision and for providing constructive suggestions during research. Hiroyuki Tsutsumi and Zakeria Shnizai are thanked for their suggestions. Ian M. Watkinson and an anonymous reviewer are also thanked for their comments, which significantly improved the manuscript.

Authors' contributions
AP is the main contributor who designed field investigation, collected the data, interpreted field data and digital elevation model, and wrote the manuscripts. PSP contributed to field data collection and wrote the manuscript. Both authors read and approved the final manuscript.

Funding
This research was funded by RC for Geotechnology LIPI.

Availability of data and materials
All the data used in this paper came from field observation and digital elevation data of Indonesia (DEMNAS) from the Geospatial Information Agency (BIG) of Indonesia (http://tides.big.go.id/DEMNAS/index.html).

Competing interests
The authors declare that they have no competing interests.

Received: 12 June 2019 Accepted: 7 January 2020
Published online: 16 January 2020

References

Bao H, Ampuero J-P, Meng L, Fielding EJ, Liang C, Milliner CWD, Feng T, Huang H (2019) Early and persistent supershear rupture of the 2018 magnitude 7.5 Palu earthquake. Nat Geosci 12:200–205. https://doi.org/10.1038/s41561-018-0297-z

Bellier O, Beaudouin T, Sébrier M, Villeneuve M, Bahar I, Putranto E, Pratomo I, Massault M, Seward D (1998) Active faulting in Central Sulawesi (Eastern Indonesia). In: Wilson P, Michel GW (eds) The Geodynamics of S and SE Asia (GEODYSSEA) Project Final Report. Postdam

Bellier O, Bourles DL, Beaudouin T, Braucher R (1999) Cosmic Ray Exposure (CRE) dating in a wet tropical domain: late quaternary fan emplacements in central Sulawesi (Indonesia). Terra Nova 11:174–180. https://doi.org/10.1046/j.1365-3121.1999.00242.x

Bellier O, Siame L, Beaudouin T, Villeneuve M, Braucher R (2001) High slip rate for a low seismicity along the Palu–Koro active fault in Central Sulawesi (Indonesia). Terra Nova 13:463–470. https://doi.org/10.1046/j.1365-3121.2001.00382.x

Bellier O, Sébrier M, Seward D, Beaudouin T, Villeneuve M, Putranto E (2006) Fission track and fault kinematics analyses for new insight into the Late Cenozoic tectonic regime changes in West-Central Sulawesi (Indonesia). Tectonophysics 413:201–220. https://doi.org/10.1016/j.tecto.2005.10.036

Bock Y, Prawirodirdjo L, Genrich JF, Stevens CW, McCaffrey R, Subarya C, Puntodewo SSO, Calais E (2003) Crustal motion in Indonesia from global positioning system measurements. J Geophys Res 108:2367. https://doi.org/10.1029/2001jb000324

Cipta A, Robiana R, Griffin JD, Horspool N, Hidayati S, Cummins PR (2017) A probabilistic seismic hazard assessment for Sulawesi, Indonesia. In: Cummins PR, Meilano I (eds) Geohazards in Indonesia: earth science for disaster risk reduction, 441st edn. Geological Society of London, London, pp 133–152

Crosetto S, Watkinson IM, Min S, Gori S, Falcucci E, Ngal NL (2018) Evidence of quaternary and recent activity along the Kyaukkyan Fault, Myanmar. J Asian Earth Sci 156:207–225. https://doi.org/10.1016/j.jseaes.2018.01.013

Daryono MR (2016) Paleoseismology of Tropical Indonesia (Cases study in Sumatran Fault, Palukoro-Matano Fault, and Lembang Fault) (Paleoseismologi Tropis Indonesia (Dengan Studi Kasus di Sesar Sumatra, Sesar Palukoro-Matano, dan Sesar Lembang)). Dissertation Doctoral Program. Institut Teknologi Bandung. Unpublished

Hall R (2002) Cenozoic geological and plate tectonic evolution of SE Asia and the SW Pacific. J Asian Earth Sci 20:353–431. https://doi.org/10.1016/S1367-9120(01)00069-4
Hall R (2012) Late Jurassic-Cenozoic reconstructions of the Indonesian region and the Indian Ocean. Tectonophysics 570–571:1–41. https://doi.org/10.1016/j.tecto.2012.04.021
Hall R (2018) The subduction initiation stage of the Wilson cycle. In: Wilson RW, Houseman GA, McCaffrey KJW, Dore AG, Buiter SJH (eds) Fifty years of the Wilson cycle concept in plate tectonics, vol 470. Geological Society, London
Hall R, Wilson MEJ (2000) Neogene sutures in eastern Indonesia. J Asian Earth Sci 18:781–808. https://doi.org/10.1016/S1367-9120(00)00040-7
Hamilton W (1979) Tectonics of the Indonesian region. USGS Professional Paper. United States Printing Office, Washington
Hinschberger F, Malod JA, Réhault JP, Villeneuve M, Royer JY, Burhanuddin S (2005) Late Cenozoic geodynamic evolution of eastern Indonesia. Tectonophysics 404:91–118. https://doi.org/10.1016/j.tecto.2005.05.005
Katili JA (1970) Large transcurrent faults in Southeast Asia with special reference to Indonesia. Geol Rundsch 59:581–600. https://doi.org/10.1007/BF01823809
Mann P, Taylor FW, Edwards RL, Ku T-L (1995) Actively evolving microplate formation by oblique collision and sideways motion along strike–slip faults: an example from the northeastern Caribbean plate margin. Tectonophysics 246:1–69. https://doi.org/10.1016/0040-1951(94)00268-E
McCaffrey R, Sutardjo R (1982) Reconnaissance microearthquake survey of Sulawesi, Indonesia. Geophys Res Lett 9:793–796. https://doi.org/10.1029/GL009i008p00793
Nugraha AMS, Hall R (2018) Late Cenozoic paleogeography of Sulawesi, Indonesia. Paleogeogr Palaeoclimatol Palaeoecol 490:191–209. https://doi.org/10.1016/j.palaeo.2017.10.033
Pakpahan S, Ngadmanto D, Masturyono M, Rohadi S, Rasmid R, Widodo HS, Susilanto P (2015) Analisis Kegempaan di Zona Sesar Palu Koro, Sulawesi Tengah. Jurnal Lingkungan dan Bencana Geologi 6:253–264
Putra PS, Aswan A, Maryunani KA, Yulianto E, Kongko W (2019) Field survey of the 2018 Sulawesi tsunami deposits. Pure Appl Geophys. https://doi.org/10.1007/s00024-019-02181-9
Rangin C, Le Pichon X, Mazzotti S, Pubellier M, Chamot-Rooke N, Aurelio M, Walpersdorf A, Quebral R (1999) Plate convergence measured by GPS across the Sundaland/Philippine Sea Plate deformed boundary: the Philippines and eastern Indonesia. Geophys J Int 139:296–316. https://doi.org/10.1046/j.1365-246x.1999.00969.x
Sassa S, Takagawa T (2019) Liquefied gravity flow-induced tsunami: first evidence and comparison from the 2018 Indonesia Sulawesi earthquake and tsunami disasters. Landslides 16:195–200. https://doi.org/10.1007/s10346-018-1114-x
Silver EA, McCaffrey R, Smith RB (1983) Collision, rotation, and the initiation of subduction in the evolution of Sulawesi, Indonesia. J Geophys Res 88:9407–9418
Socquet A, Simons W, Vigny C, McCaffrey R, Subarya C, Sarsito D, Ambrosius B, Spakman W (2006) Microblock rotations and fault coupling in SE Asia triple junction (Sulawesi, Indonesia) from GPS and earthquake slip vector data. J Geophys Res Solid Earth 111:B08409. https://doi.org/10.1029/2005JB003963
Socquet A, Hollingsworth J, Pathier E, Bouchon M (2019) Evidence of supershear during the 2018 magnitude 7.5 Palu earthquake from space geodesy. Nat Geosci 12:192–199. https://doi.org/10.1038/s41561-018-0296-0
Stevens C, McCaffrey R, Bock Y, Genrich J, Endang Subarya C, Puntodewo SSO, Fauzi Vigny C (1999) Rapid rotations about a vertical axis in a collisional setting revealed by the Palu fault, Sulawesi, Indonesia. Geophys Res Lett 26:2677–2680. https://doi.org/10.1029/1999GL008344
Sukamto RAB, Sumadirdja H, Suptandar T, Hardjoprawiro S, Sudana D (1973) Reconnaissance Geological Map of the Palu Quadrangle, Sulawesi. Geological Research and Development Centre, Bandung
Takagi H, Pratama MB, Kurobe S, Esteban M, Aránguiz R, Ke B (2019) Analysis of generation and arrival time of landslide tsunami to Palu City due to the 2018 Sulawesi earthquake. Landslides 16:983–991. https://doi.org/10.1007/s10346-019-01166-y
Tjia HD (1978) Active Faults in Indonesia. Bull Geol Soc Malaysia 10:73–92
Villeneuve M, Gunawan W, Cornee J-J, Vidal O (2002) Geology of the central Sulawesi belt (eastern Indonesia): constraints for geodynamic models. Int J Earth Sci 91:524–537. https://doi.org/10.1007/s005310100228
Walpersdorf A, Vigny C, Subarya C, Manurung P (1998) Monitoring of the Palu–Koro Fault (Sulawesi) by GPS. Geophys Res Lett 25:2313–2316
Watkinson IM, Hall R (2017) Fault systems of the eastern Indonesian triple junction: evaluation of Quaternary activity and implications for seismic hazards. In: Cummins PR, Meilano I (eds) Geohazards in Indonesia: earth Science for Disaster Risk reduction, vol 441. Geological Society of London, London, pp 71–120
Wu JE, McClay K, Whitehouse P, Dooley T (2009) 4D analogue modelling of transtensional pull-apart basins. Mar Pet Geol 26:1608–1623. https://doi.org/10.1016/j.marpetgeo.2008.06.007
Zhang P, Burchfiel BC, Chen S, Deng Q, Zhang P, Burchfiel BC, Chen S (1989) Extinction of pull-apart basins extinction of pull-apart basins. Geology 17:814–817. https://doi.org/10.1130/0091-7613(1989)017%3c0814

Publisher's Note